Efficient electrocatalyst of α-Fe_2O_3 nanorings for oxygen evolution reaction in acidic condition

Xiaolei Liang,[a, b] Jinmei Qian,[b] Yonggang Liu,[b] Zhengmei Zhang,[b] Daqiang Gao[b]*

[a]Department of obstetrics and gynecology, the First Hospital of Lanzhou University, Key Laboratory for Gynecologic Oncology Gansu Province, China.

[b]Key Laboratory for Magnetism and Magnetic Materials of MOE, Key Laboratory of Special Function Materials and Structure Design of MOE, Lanzhou University, Lanzhou 730000, China

*E-mail: gaodq@lzu.edu.cn

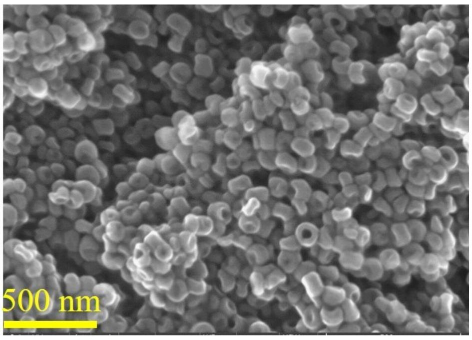

Figure S1. The SEM image of α-Fe_2O_3 NRs.

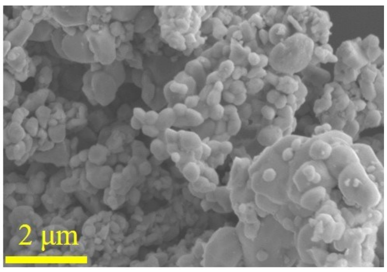

Figure S2. The HRTEM images of bulk α-Fe_2O_3.

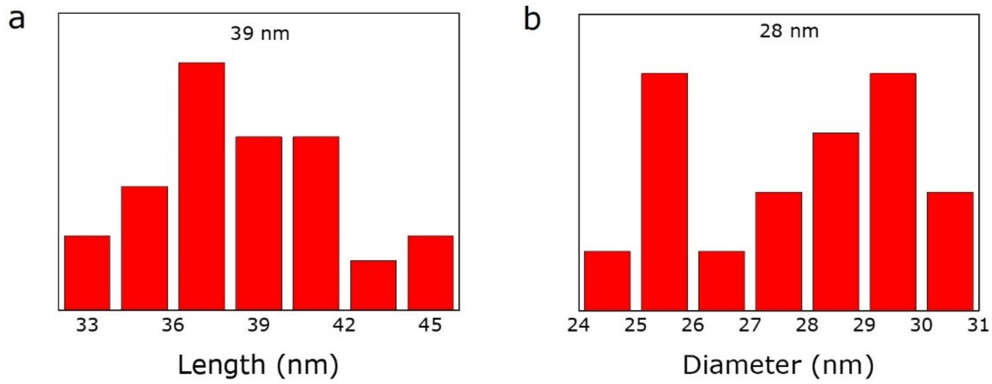

Figure S3. The length (a) and dimeter (b) of nanorings of α-Fe_2O_3 NRs.

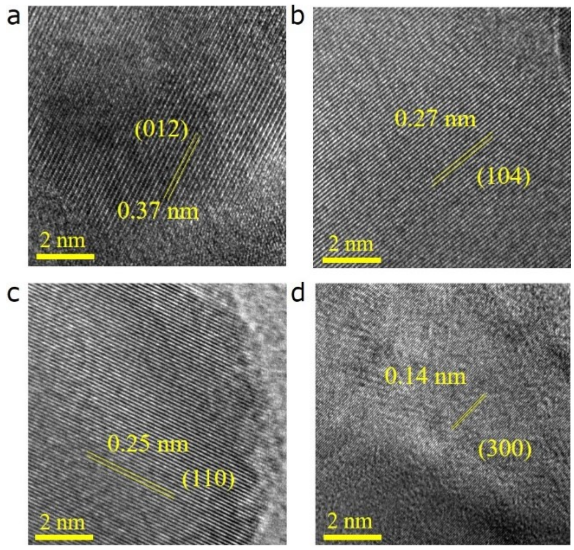

Figure S4. The HRTEM images of α-Fe_2O_3 NRs with perpendicular to (a-c) and along the nanoring direction (d).

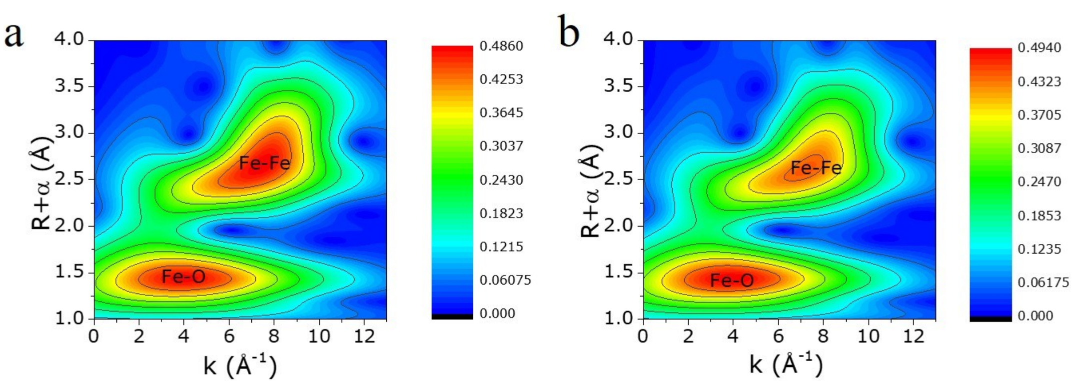

Figure S5: WT for the k^3-weighted EXAFS signals for (a) bulk α-Fe_2O_3 and (b) α-Fe_2O_3 NRs.

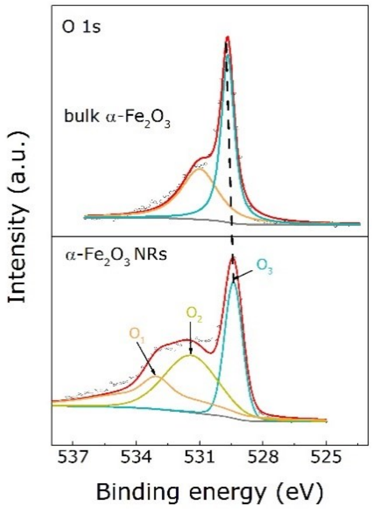

Figure S6. The XPS results of O 1s for bulk α-Fe_2O_3 and α-Fe_2O_3 NRs, where the peaks of bulk α Fe_2O_3 shift to higher binding energy (～0.3 eV).

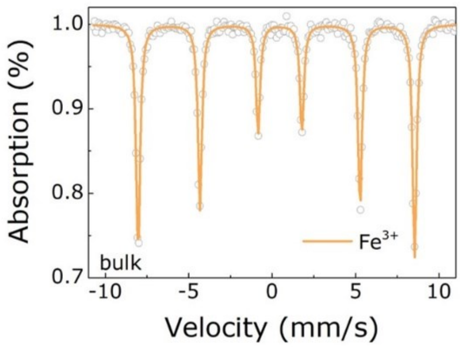

Figure S7. The Mossbauer spectrum of bulk α-Fe_2O_3.

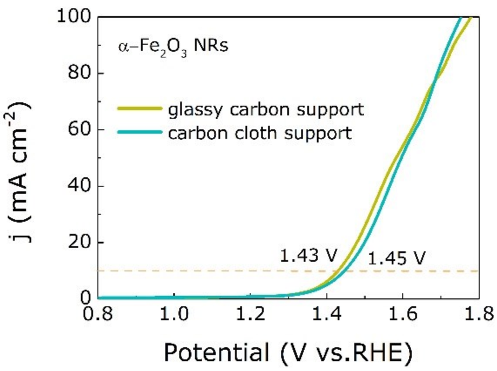

Figure S8. LSV curves of α-Fe_2O_3 NRs electrocatalyst based on glassy carbon support and carbon cloth support.

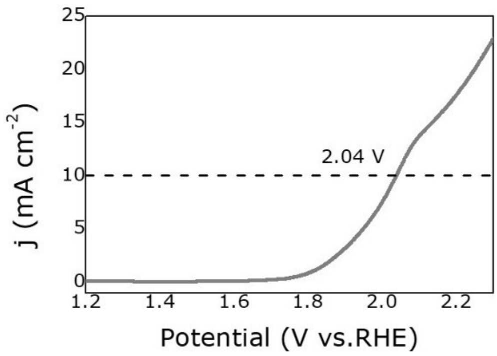

Figure S9. The LSV curve of α-Fe_2O_3 NRs electrocatalyst free substrate.

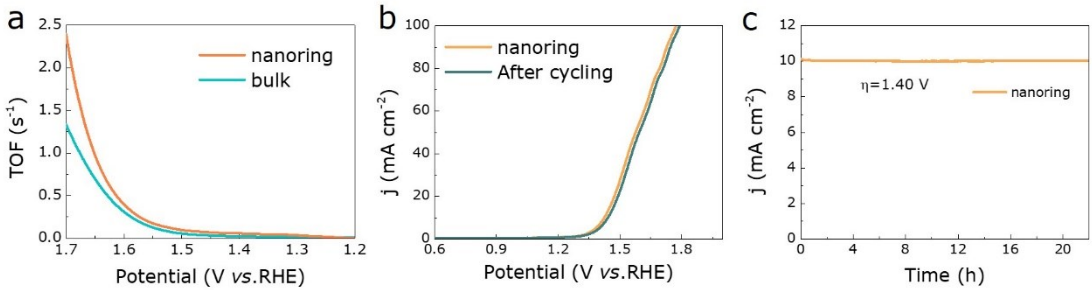

Figure S10. (a) The TOF curves of the α-Fe_2O_3 NRs and bulk α-Fe_2O_3 ($TOF = j \times S/4 \times F \times n$, where j is the measured current density, S is the electrode geometric area, F is the Faraday's constant of 96485.3 C mol^{-1}, n is the moles of coated Fe atom on the electrode). (b) LSV curves of α-Fe_2O_3 NRs before and after stability test of 10000 cycles and (c) I-t curve of α-Fe_2O_3 NRs.

Table S1. EXAFS fitting parameters at the Fe K-edge for bulk α-Fe_2O_3 and (b) α-Fe_2O_3 NRs.（S_0^2=0.70）

Sample	Shell	N^a	R(Å)^b	$\sigma^2\times10^3$(Å^2)^c	ΔE_0 (eV)^d	R factor
bulk α-Fe_2O_3	Fe-O	6.0±1.3	1.96±0.02	12.0±2.5	-7.9±3.0	0.010
	Fe-Fe	6.7±1.1	2.99±0.01	9.2±1.3	3.1±1.7	
	Fe-Fe	3.0±0.9	3.67±0.01	2.9±1.6	6.7±1.1	
α-Fe_2O_3 NRs	Fe-O	6.2±1.5	1.96±0.02	12.0±2.7	-9.0±3.3	0.010
	Fe-Fe	6.8±1.1	3.00±0.01	8.6±1.2	3.3±1.7	
	Fe-Fe	3.3±0.9	3.67±0.01	2.5±1.5	-8.9±2.6	

^aN: coordination numbers; ^bR: bond distance; $^c\sigma^2$: Debye-Waller factors; ^{d} ΔE_0: the inner potential correction. R factor: goodness of fit.

Table S2. The Mössbauer spectra related parameters.

Sample	Isomer shift (mm)	Magnetic field (T)
Bulk α-Fe_2O_3	0.36432	50.40895
α-Fe_2O_3 NRs	0.36387	50.39407

Table S3. The electrocatalytic OER performances of some reported electrocatalysts.

Electrocatalyst	electrolyte	Potential (V) at 10 mA cm^{-2}	Tafel slope (mV dec^{-1})	TOF (s^{-1})	Reference
Fe_2O_3-(012)-O	1 M NaOH	1.53	51.8	0.197	[1]
Fe_2O_3-(104)	1 M NaOH	1.62	62.5	0.049	[1]
FC-2	0.1 M KOH	1.56	45	/	[2]
α-Fe_2O_3@g-C_3N_4-NCs	0.5 M KOH	1.65	280	/	[3]
α-Fe_2O_3 NPs	0.5 M KOH	1.76	320	/	[3]
CM/TiO_{2-x} /CP	1 M KOH	1.47	67.1	/	[4]
NiFeSe@NiSe|O@CC	1 M KOH	1.50	63.2	/	[5]

FeN_x/NF/EG	0.5 M H_2SO_4	1.82	129	/	[6]
Fe-Fe_2O_3	pH=0	2.14	/	/	[7]
Fe-Co/Fe_2O_3	pH=0	2.18	/	/	[7]
Co-Co/Fe_2O_3	pH=0	1.86	/	/	[7]
$Rh_{22}Ir_{78}$ NPs	0.5 M H_2SO_4	1.52	101	5.1	[8]
Mn-RuO_2	0.5 M H_2SO_4	1.39	42.9	0.4	[9]
α-Fe_2O_3 NRs	1 M HCl	1.43	138	2.3	This work
Bulk α-Fe_2O_3	1 M HCl	1.89	350	1.3	This work

Reference

1 H. Wu, T. Yang, Y. H. Du, L. S. Shen, G.W. Ho , *Adv. Mater.*, 2018, **30**, 1804341

2 T. W. Odedairo, X. C. Yan, K. Ostrikov, Z. H. Zhu, *Adv. Mater.*, 2017, **29**, 1703792.

3 O. Alduhaish, M. Ubaidullah, et. al, *Adv. Mater.*, 2019, **9**, 14139.

4 F. L. Meng, G. Yilmaz, T. P. Ding, M. M. Gao, and G. W. Ho, Adv. Mater., 2019, **31**, 1903605.

5 G. Yilmaz, C. F. Tan, Y. F. Lim, and G. W. Ho, Adv. Energy Mater., 2018, 1802983

6 C. J. Lei, et al. *Adv. Energy Mater.,* 2018, **8**, 1801912.1-1801912.7.

7 N. Lu, W. H. Zhang, X. J. Wu, Chin. J. Chem. Phys. 2017, **30**.

8 H. Y. Guo, et al. *ACS Nano*, 2019, **13**, 13225-13234.

9 S. Chen, et al. *ACS Catalysis.* 2019, **10**, 1152-1160.